Optical coupling mechanisms in quantum well infrared photodetectors

Sumith Bandara, Sarath Gunapala, John Liu, Winn Hong and Jin Park

Center for Space Microelectronics Technology
Jet Propulsion Laboratory
California Institute of Technology
Pasadena, CA 91109

ABSTRACT

Light coupling systems, such as gratings are required because Quantum Well Infrared Photodetectors do not respond to normal incident light due to the quantum mechanical selection rules associated with intersubband transitions. The resolution of the photolithography and accuracy of the etching become key issues in producing smaller grating feature sizes especially in shorter wavelengths. An enhancement factor of three due to 2D periodic grating fabricated on a QWIP structure was observed. Variation of the enhancement factor with groove depth and feature size of the grating can be theoretically explained.

Keywords: Quantum Wells, intersubband, infrared, detectors, grating

INTRODUCTION

Development of the hand-held long wavelength infrared (LWIR)[1,2] camera at Jet Propulsion Laboratory demonstrated the potential of Quantum Well Infrared Photodetector (QWIP) technology for fabrication of a simple and highly sensitive infrared imaging system. This camera features a $GaAs/Al_xGa_{1-x}As$ bound-to-quasibound multi-quantum well (MQW) focal plane array (FPA) hybridized to an Amber 256x256 direct injection CMOS readout multiplexer. The QWIP FPA offers high detector-to-detector uniformity, low noise, ease of fabrication and exhibits a cutoff wavelength of 8.9 μm and noise-equivalent temperature difference of 25 mK or less. Due to its higher sensitivity, higher uniformity, higher yield, and lower cost, there is a great interest in $GaAs/Al_xGa_{1-x}As$ based QWIP technology.

QWIPs do not absorb radiation incident normal to the surface since the light polarization must have an electric field component normal to the superlattice (growth direction) to be absorbed by the confined carriers[3]. When the incoming light contains no polarization component along the growth direction, the matrix element of the interaction vanishes (i.e., $\vec{\varepsilon}.\vec{p}_z = 0$ where $\vec{\varepsilon}$ is the polarization and $\vec{p}_z$ is the momentum along z direction). As a consequence, these detectors have to be illuminated through a 45" polished facet[3]. Clearly, this illumination scheme limits the configuration of detectors to linear arrays and single elements. For imaging, it is necessary to be able to couple light uniformly to two dimensional arrays of these detectors.

QWIP LIGHT COUPLING METHODS

Several different monolithic grating structures, such as linear gratings[4,5], two-dimensional (2-D) periodic gratings[6-8], and random-reflectors[9,10] have been demonstrated for efficient light coupling to QWIPs, and has made two dimensional QWIP imaging arrays 1,2 feasible. See Fig. 1. These gratings deflect the incoming light away from the direction normal to the surface, enabling intersubband absorption. These gratings were made of metal on top of each detector or crystallographically groove etched through a cap layer on top of the MQW structure. Normal incident light-coupling efficiency comparable to the light coupling efficiency of a 45" polished facet illumination was demonstrated using linear gratings[4,5].

Detailed theoretical analysis[7] has been carried out on both linear and 2-D periodic gratings for QWIPs. In 2-D gratings, the periodicity of the grating repeats in two perpendicular directions on the detector plane (Fig. I a), leading to the absorption of both polarizations of incident IR radiation. Also, experiments have been carried out for two-dimensional grating coupled QWIP detectors designed for wavelengths λ -9 μm[6] and λ - 16 - 17 μm[8]. A factor of 2-3 responsivity enhancement relative to the standard 45" polished facet illumination was observed for large area mesas (500 μm x 500 μm) with total internal reflection optical cavity which can be created with an additional AlGaAs layer[6,7] or with a thinned substrate. This optical cavity is responsible for about an extra enhancement factor of two due to the total internal reflection from the AlGaAs layer or from the thinned substrate (Fig. l-b, I-c).

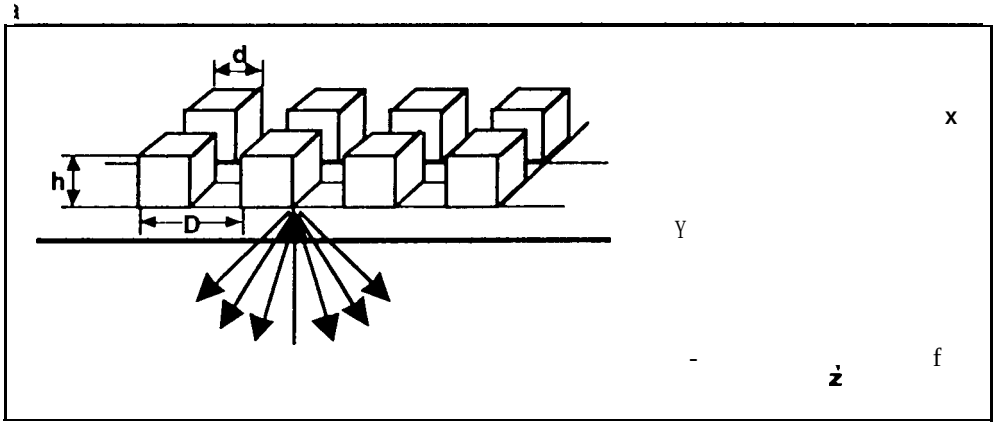

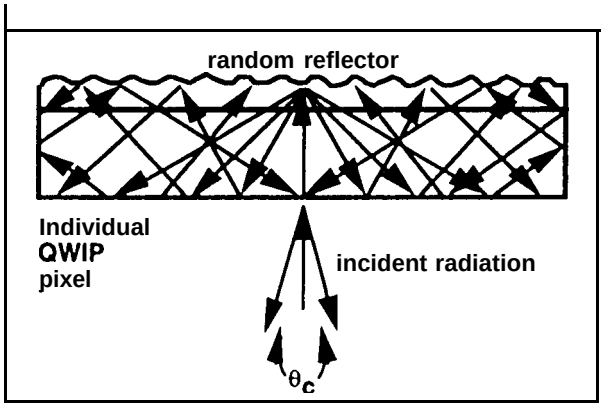

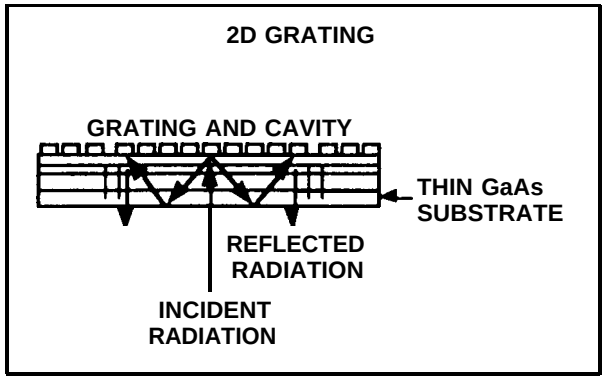

Fig. I (a) Schematic side view of a thin QWIP pixel with a 2-D periodic grating. All the incident radiation escape after the second reflection from the grating surface. (b) Schematic side view of a thin QWIP pixel with a random grating reflector. Ideally all the radiation is trapped except for a small fraction which escapes through the escape cone. (c) Schematic diagram of cross grating specifications. The grating features are spaced periodically along the x and y directions.

Random reflectors have demonstrated excellent optical coupling for individual QWIPs as well as for large area focal plane arrays[9,10]. It has been shown that many more passes of IR light (Fig 1-c), and significantly higher absorption, can be achieved with a randomly roughened reflecting surface. By careful design of surface texture randomization (with three level random reflector), an enhancement factor-of-eight in responsivity compared to 45° illumination was demonstrated experimentally[9]. The random structure on top of the detector prevents the light from being Ltitl'ratted normally backward after the second bounce as happens in the case of 2-D periodic grating. See Fig 1, Naturally, thinning down the substrate enables more bounces of light and therefore higher responsivity[9].

All these gratings were fabricated on the detectors by using standard photolithography and selective dry etching. The advantage of the photolithograpic process is its ability to accurately control the feature size and to preserve the pixel-to-pixel uniformity, which is a prerequisite for high-sensitivity imaging focal plane array. However the resolution of the photolithography and the accuracy of etching processes become key issues in producing smaller grating feature sizes. These feature sizes are proportionally scaled with the peak response wavelength of the QWIP. It is important to note that for any given wavelength random grating requires much smaller feature sizes than two dimensional periodic gratings. Figures 2(a) and 2(b) show random reflectors on a pixel of, 15 μm cutoff 128x128 and 9 μm cutoff 256x256 QWIP FPAs respectively. The minimum feature size of the random reelectors of 15 μm and 9 μm cutoff FPAs were 1.25 and 0.6 μm respectively. As shown on Fig. 2(b) the random reflectors of the 9 μm cutoff FPA were less sharp and had fewer scattering centers compared to Fig. 2(a) and this is due to the difficulties associated with sub-micron photolithography. These less sharp features in random gratings lowered the light coupling efficiency than expected. Thus, it could be advantageous to utilize a 2-D periodic grating for light coupling in shorter wavelength QWIPs.

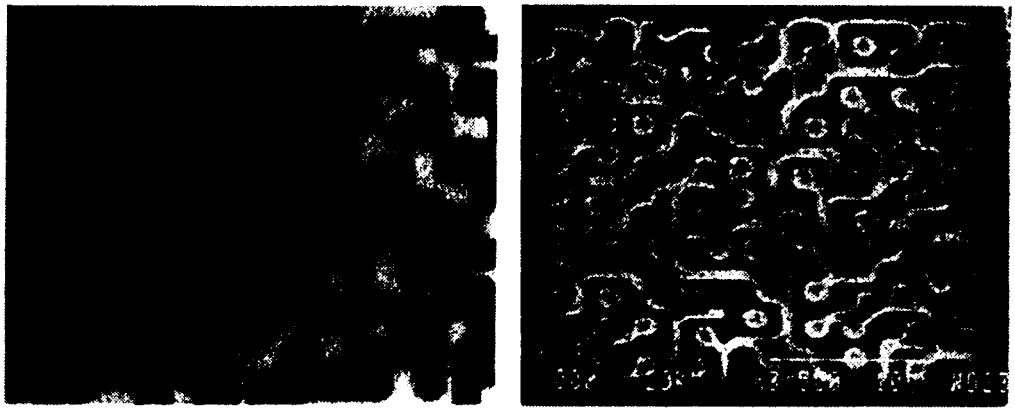

a b

Fig. 2 (a) Two level random reflectors on a pixel (38x38 μm^2) of' 15 μm cutoff 128x128 QWIP FPA The rninirnum feature size is 1.25 μm. (b) Two level random reflectors on a pixel (28x28 μm^2) of 9 μm cutoff 256x256 QWIP. The minimum feature size is 0.6 μm. This random reflector has fewer scattering centers compared to Fig. 2(a) due to the difficulties associated with sub-micron photolithography.

2-1) GRATING TEST STRUCTURES

Six different 2-D grating periods (D) were fabricated on a standard QWIP structure designed to perform at peak wavelength, λ_p -8.5 μm. The device structure consists of 50 periods, each period containing a 45 A well of GaAs and 500 A barrier of $Al_{0.3}Ga_{0.7}As$, sandwiched between top and bottom contact layers doped n = 5x 10^{17} cm^{-3}, grown on a semi-insulating GaAs substrate by molecular beam epitaxy (MBE). The cap layer on top of a stop-etch layer was grown *in situ* on top of the device structure to fabricate the light coupling 2-D grating structure. In order to fabricate three QWIP samples with three different grating groove depths h (Fig. I (c)), the top cap layer of each sample was thinned down to a different thickness by chemical etching. After 2-D gratings were defined by the photolithography and dry etching, these samples were processed into 200 x 200 μm^2 and 400 x 400 μm^2 mesa test structures. Then the 2-D grating reflectors on the top of the detectors and bottom contact layers were covered by Au/Ge and Au for Ohmic contact and reflection respectively. As a control sample, a standard 45° edge polished fa cet sample was also fabricated from the original QWIP wafer

EXPERIMENTAL RESULTS

The responsivity spectra of these detectors were measured using a 1000 K blackbody source and a grating monochromator. The absolute peak responsivities (R_p) of these detectors were measured using a calibrated blackbody source. Detectors of the control sample were illuminated through a 45" polished facet and all the grating samples were illuminated normal to the detector plane. The normalized responsivity spectrum for grating samples (with one groove depth) and for the standard 45" sample are shown in Fig. 3. Note the normalized spectral peak shifts from 7.5 μm to 8.8 μm as the grating period increases from D = 2.2pm to 3.2 μm. These measurements were repeated with all 19 samples (i.e., six different grating parameters for each groove depth and one 45" sample), The grating peak wavelength λ_{gp} (where the grating enhancement is maximized) and the peak enhancement is (enhancement at λ_{gp}) associated with each grating period was obtained by normalizing the absolute spectral responsivity of the grating detectors relative to the 45^0 detector sample. Fig. 4 shows the variation of the grating peak wavelength with grating period for samples with three different groove depths. As expected from the theory, λ_{gp} linearly depends on the grating period and it is independent of the groove depth of the grating.

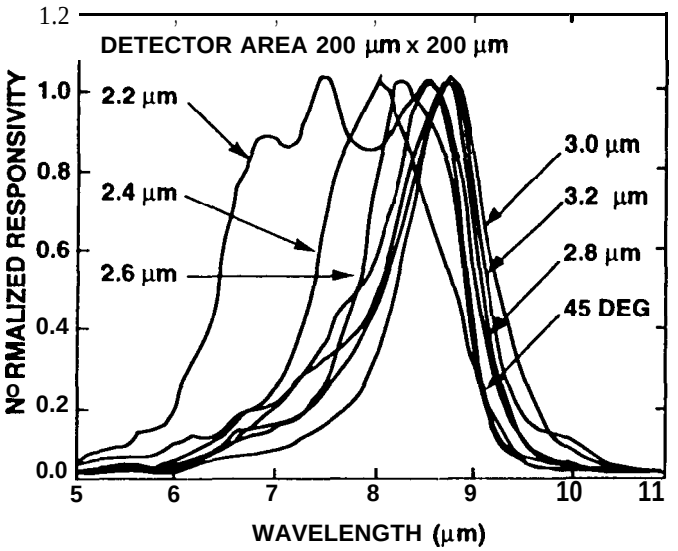

Fig. 3 Measured normalized responsivity spectra as a function of grating period D for D = 2.2 -3.2 μm. The bold curve represent responsivity spectra same QWIP with 45(' polished edge.

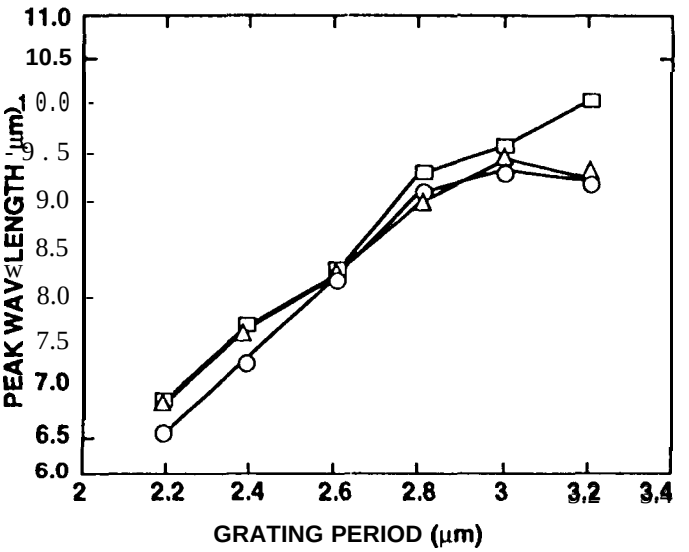

Fig. 4 Measured grating peak wavelength λ_{gp} vs. the grating period for samples with three different groove depths h.

Figure 5 shows experimental responsivity enhancement due to 2-D grating at λ_{gp} for each grating period with different groove depths. Only one sample shows enhancement up to a factor of 3.5 (curves a and b in Fig. 5) depending on the grating period, while the other two samples show no enhancement and no dependence on the grating period. This enhancement factor of about three was measured in a similar (same gratings and groove depth) sample with different detector area. Scanning Electron Microscopic (SEM) pictures of two samples, associated with curve c and d of Fig. 5, clearly show some distortion in the features of the gratings. This can be attributed to the partial contact between the grating mask and the wafer during the photolithography. Although the grating periods, were unchanged from the designed value, feature sizes, (see Fig. I-a) were reduced during the processing.

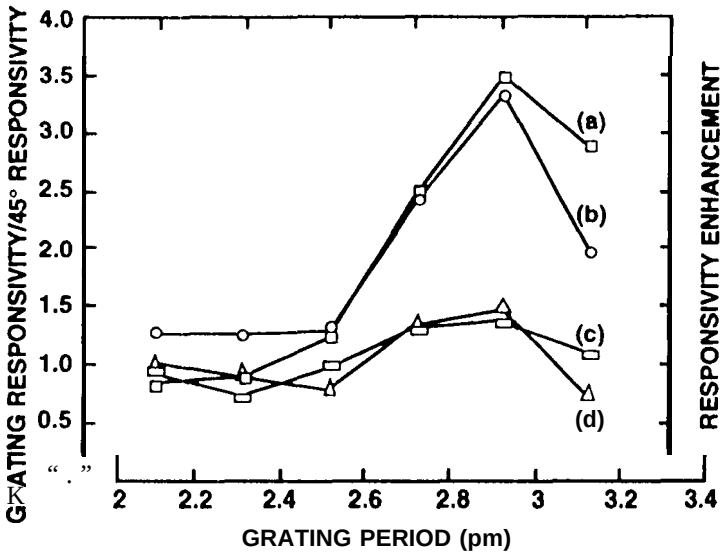

Fig. 5 The experimental responsivity enhancement at λ_{gp} for each grating period with different groove depths. Curves a and b represent gratings with same groove depth but different in detector area (a - 200x200 μm^2 and b - 400x400 μm^2). Curve c and d represent 200x200 μm^2 area detectors with different groove depths.

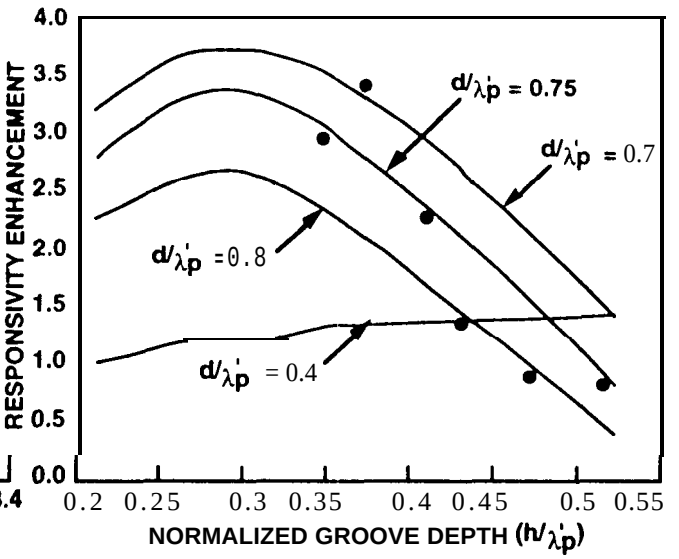

Fig. 6 The experimental data and theoretical comparison for responsivity enhancement in 2-D periodic grating coupled QWIP. Theoretical curves were plotted as a function of groove depth, h for different feature sizes d normalized to characteristic grating peak wavelength in GaAs, λ_{gp}'. Feature sizes d for each grating were obtained using SEM pictures of each grating. Also, shown that a responsivity enhancement at lower d/ λ_{gp}' which is the case in two samples associated with curve c and d in the Fig. 5.

THEORETICAL ANALYSIS

In order to explain responsivity enhancement shown in Fig. 5 (curve a and b), theoretical analysis of 2-D periodic gratings were carried out based on modal expansion method [1,7] in which, electric and magnetic field vectors are matched at the boundary (z = O plane, Fig. la) between the diffracted field region and rectangular cavity region The field vectors in the diffracted field region ($z > 0$ in Fig. 1a), and inside the cavities ($z < 0$ in Fig. l-a), are expressed in terms of diffracted "orders", and guided vector "modes", respectively. Each of these diffracted "orders" is associated with a plane wave propagating in a discrete direction which is specified by a pair of integers (p,q) due to the double periodicity of the grating structure. The guided vector "mode" inside the cavity means a vector field not only satisfying Maxwell's equations, but also boundary conditions appropriate to the geometry of the cavity. These modes are also specified by pair of integers (n,m) due to rectangular nature of the grating cavity. The resulting system of equations are then solved for diffracted plane wave amplitudes by limiting the diffracted orders up to the first set of orders ($p^* + q^2 \leq 1$), or second set of orders ($p^* + q^2 \leq 2$). The efficiencies of the diffracted order, i.e., the amplitude of the electric field vector E_{pq} of the (p,q)th diffracted order can then be calculated as a function feature size, d and groove depth h of the grating.

Fig. 6 shows the experimental data and theoretical comparison for responsivity enhancement due to 2-D periodic gratings. Theoretical curves were plotted as a function of groove depth (h) for different feature sizes (d) normalized to characteristic grating peak wavelength in GaAs, λ_{gp}(GaAs). Feature sizes d for each grating were obtained using SEM pictures of each grating. Although the designed normalized feature size d/ λ_{gp}(GaAs) is the same for all the gratings, SEM measurements show variations. These variations can be attributed to the limitations of device fabrication processes such as photolithography and metal ization. Also, Fig. 6 shows that at lower d/λ_{gp}(GaAs), responsivity enhancement is independent of groove depth ot'the grating, which is the case in two samples associated with curves c and d in Fig. 5.

SUMMARY

In summary, we have observed an enhancement factor of' three due to 2D periodic grating fabricated on QWIP structure. Variation of the enhancement factor with groove depth and feature size of the grating can be theoretically explained. However the resolution of the photolithography and accuracy of the etching become key issues in producing smaller grating feature sizes especially in shorter wavelengths. Unlike random reflectors the light coupling efficiency of two dimensional (2-D) gratings strongly depends on the wavelength and thus exhibits narrow band width spectral responses. Therefore, 2-D gratings can be utilized to select narrow spectral bands in multi color QWIP cameras. A set of 2-D grating parameters optimized for given spectral band can be obtained by using the modal expansion method.

ACKNOWLEDGMENTS

The research described in this paper was performed by the Center for Space Microelectronics Technology, Jet Propulsion Laboratory, California Institute of Technology, and was jointly sponsored by the Ballistic Missile Defense Organization/Innovative Science and Technology Office, and the National Aeronautics and Space Administration, Office of Space Science.

REFERENCES

1. S. D. Gunapala, J. K. Liu, J. S. Park, M. Sundaram, C. A. Shott, T. Holter, T. L. Lin, S. T. Massie, P. D. Maker, R. E. Muller, and G. Sarusi, IEEE Trans. Ele. Devices, vol. 44,51 (1997).

2. S. D. Gunapala, J. K. Liu, M. Sundaram, S. V. Bandara, C. A. Shott, T. Helter, P. D. Maker, and R. E. Muller, SPIE Proceedings, V 2746, 124(1996).

3. S. D. Gunapala and K. M. S. V. Bandara, Physics of Thin Films, Academic Press, vol. 21, 113 (1995), *and references there in.*

4. K. W. Goossen, S. A. Lyon, J. Appl. Phys, vol. 63,5149 (1988).

5. G. Hansain, B. F. Levine, C. G. Bethea, R. A. Logan, J. Walker, and R. J. Malik, Appl. Phys. lett., vol. 54, 2515 (1989).

6. J. Y. Andersson and L. Lundqvist, Appl. Phys, Lett. vol. 59,857 (1991).

7. J. Y. Andersson, L. Lundqvist and Z. F. Paska, J. Appl. Phys. vol. 71,3600 (1991).

8. G. Sarusi, B. F. Levine, S. J. Pearton, K. M. S. V. Bandara, R. E. Leibenguth, and J. Y. Andersson J. Appl. Phys., vol. 76, 4989 (1994).

9. B. Xing, and H. C. Liu, J. Appl. Phys., vol. 80, 1214 (1996).

10. G. Sarusi, B. F. Levine, S. J. Pearton, K. M. S. V. Bandara, and R. E. Leibenguth, *Appl. Phys. Lett., vol. 64,* pp. 960-962, (1994).

11. R. Petit, Electromagnetic Theory of Gratings, p.227, Springer-Verlag Berlin (1980).